Chemical Vapor Deposition of $MgAl_2O_4$ Thin Films Using Different Mg−Al Alkoxides: Role of Precursor Chemistry

Sanjay Mathur,* Michael Veith,* Thomas Ruegamer, Eva Hemmer, and Hao Shen

Leibnitz Institute of New Materials, CVD Division, D-66123 Saarbruecken, Germany

Received November 12, 2003. Revised Manuscript Received January 12, 2004

We have studied the chemical and material aspects of molecular precursor-derived materials taking the example of the spinel $MgAl_2O_4$. Three Mg−Al alkoxides, $[MgAl_2(OPr^i)_8]$, $[MgAl_2(OBu^t)_8]$ and $[MgAl_2(OBu^t)_4H_4]$ were used as single molecular precursors in the gas-phase synthesis of the $MgAl_2O_4$ films. A comparative evaluation of the growth rates, morphology, microstructure, average particle size, consistency of elemental ratio, and carbon contamination in the films shows that material properties of the CVD deposits are a function of the chemical design of the precursor molecule. The intrinsic precursor properties (physical state, vapor pressure, decomposition temperature, etc.) can be tuned by a judicious choice of ligand(s) or their combination. For instance, $[MgAl_2(OPr^i)_8]$ based on isopropoxide ligands displays a potential to oligomerize upon aging due to the presence of an unsaturated metal center (Mg) in the precursor framework. Nevertheless, the liquid state of $[MgAl_2(OPr^i)_8]$ provides adequate vapor pressure for growing high-quality spinel films. In contrast, the bulkier *tert*-butoxide groups in $[MgAl_2(OBu^t)_8]$ make it thermally and structurally more stable, however causing a lower vapor pressure and higher decomposition temperature. $[MgAl_2(OBu^t)_4H_4]$ exhibits substantially high vapor pressure but the films obtained contain small amounts of residual organics, although the combination of hydride and *tert*-butoxide ligands in $[MgAl_2(OBu^t)_4H_4]$ induces a designed ligand elimination, based on the β-hydride elimination. Despite the fact that microstructured $MgAl_2O_4$ films with sufficient crystallinity and a columnar microstructure could be obtained by tuning the growth parameters of the three Mg−Al compounds, this study underscores the importance of precursor chemistry in designing an efficient CVD process.

Introduction

Magnesium aluminum spinel, $MgAl_2O_4$, is a material of choice for refractory and structural applications under high-temperature conditions, because of its high melting point (2135 °C), mechanical strength, and chemical resistance.[1,2] The outstanding material properties of spinel make it a promising replacement for traditional chromite-based refractories, which is necessary because of the environmental and health hazards of Cr^{6+} species.[3] In addition, Mg−Al spinel films exhibit potential as thermal barrier coatings (TBCs) for the blades and vanes in the hot section components of gas turbines.[4] Magnesium aluminate films are also finding applications as buffer layers for the growth of oxide superconductors[5] and as humidity sensors.[6]

Given the wide range of technological interests, $MgAl_2O_4$ has been prepared, both in powder and film form, using different techniques such as solid-state reactions or high-energy milling of component oxides,[7] complexing of metal ions by chelating ligands and subsequent thermal treatments,[8] coprecipitation of Mg and Al hydroxides,[9] hydrothermal processing of metal salts,[10] sol−gel processing of alkoxide precursors,[11] and spray pyrolysis of metal−organic derivatives.[12] In the context of thin film deposition, thermal and plasma-enhanced chemical vapor deposition have been used to grow $MgAl_2O_4$ thin films from heterometallic Mg−Al compounds used as single-source precursors.[12−15] We report here on the gas phase behavior of three hetero-metal alkoxides, namely $[MgAl_2(OPr^i)_8]$,[16] $[MgAl_2-$

* Authors to whom correspondence should be addressed. Phone: 0049-681-9300-338. Fax: 0049-681-9300-279. E-mail: smathur@inm-gmbh.de.

(1) Bhaduri, S.; Bhaduri, S. B. *Ceram. Int.* **2002**, *28*, 153.
(2) Mitchell, T. E. *J. Am. Ceram. Soc.* **1999**, *82*, 3305.
(3) Marvin, C. G. *Am. Ceram. Soc. Bull.* **1993**, *72* (6), 66.
(4) Wahl, G.; Nemetz, W.; Giannozzi, M.; Rushworth, S.; Baxter, D.; Archer, N.; Cernuschi, F.; Boyle, N. *J. Eng. Gas Turbines Power* **2001**, *123*, 520.
(5) Ogata, H.; Hanfusa, H.; Yoneda, K. *J. Cryst. Growth* **1989**, *95*, 500.
(6) Mattogno, G.; Righini, G.; Montesperelli, G.; Traversa, E. *J. Mater. Res.* **1994**, *9*, 1426.
(7) Schreyeck, L.; Wlosik, A.; Fuzellier, H. *J. Mater. Chem.* **2001**, *11*, 483.
(8) Labouthee, A.; Wongkasemjit, S.; Traversa, E.; Laine, R. M. *J. Eur. Ceram. Soc.* **2000**, *20*, 91.
(9) Li, J. G.; Ikegami, T.; Lee, J. H.; Mori, T.; Yajima, Y. *J. Eur. Ceram. Soc.* **2001**, *21*, 139.
(10) Byrappa, K.; Yoshimura, M. *Handbook of Hydrothermal Technology: Technology for Crystal Growth and Materials Processing*; William Andrew, New York, 2001.
(11) Rai, J.; Mehrotra, R. C. *J. Non-Cryst. Solids* **1993**, *152*, 118.
(12) Meese-Marktscheffel, J. A.; Fukuchi, R.; Kido, M.; Tachibana, G.; Jensen, C. M.; Gilje, J. W. *Chem. Mater.* **1993**, *5*, 755.
(13) Zhang, J.; Stauf, G. T.; Gardiner, R.; Buskirk, P. V.; Steinbeck, J. *J. Mater. Res.* **1994**, *9*, 1333.
(14) Koh, W.; Ku, S. J.; Kim, Y. *Chem. Vap. Dep.* **1998**, *4*, 192.
(15) (a) Veith, M.; Altherr, A.; Wolfanger, H. *Chem. Vap. Dep.* **1999**, *5*, 87. (b) Winter, R.; Quinten, M.; Dierstein, A.; Hempelmann, R.; Altherr, A.; Veith, M. *J. Appl. Crystallogr.* **2000**. *33*, 507.

10.1021/cm0311675 CCC: $27.50
Published on Web 03/04/2004

$(OBu^t)_8]$,[17] and $[MgAl_2(OBu^t)_4H_4]$[15] in a low-pressure CVD reactor. For a comparative evaluation of the decomposition chemistry of the precursor molecules, the three compounds have been examined on the same CVD reactor and under identical experimental conditions. The application of single molecular precursors in gas phase methods offers the advantage of a controlled stoichiometry and crystallization of the solid phase at relatively low temperatures.[18−26] In addition, the process parameters such as precursor delivery and concentration adjustment are reduced (simplified), when compared to a multicomponent CVD process. $MgAl_2O_4$ films have been grown by conventional CVD using $MgCl_2$, Al, HCl, CO_2, and H_2 as starting materials and carrier gases, however high growth temperature (980 °C) and poor stoichiometry in the film were the major shortcomings.[27] Despite the promises of molecular precursors, their application is seen with skepticism mainly due to lack of (i) suitable precursor compounds, especially for bimetallic oxides,[28] with adequate vapor pressure, and (ii) evidence for the conservation of stoichiometry present in the molecular source, during the CVD process (*proof of the concept*). In addition, systematic studies on precursor chemistry and its relation to the final material properties are missing. We focus here on the chemical behavior of different source reagents and their influence on stoichiometry, crystallization temperature, grain size, microstructure, roughness, and organic contamination, in the resulting spinel films.

Experimental Section

(i) Chemicals. The syntheses of alkoxide precursors and other experimental manipulations were performed in a modified Schlenk type vacuum assembly, taking stringent precautions against atmospheric moisture. Solvents were purified by standard methods and stored over appropriate desiccating agents. Anhydrous $MgCl_2$ and $AlCl_3$ (Aldrich) were dried in a vacuum (110 °C/10^{-2} Torr) and analyzed for chlorine contents before use. The Mg−Al alkoxide derivatives, $[MgAl_2(OPr^i)_8]$, $[MgAl_2(OBu^t)_8]$, and $[MgAl_2(OBu^t)_4H_4]$ were prepared following published procedures[12,15,29] and have been abbreviated as **MA1**, **MA2**, and **MA3**, respectively, in the figures and captions. The compounds were purifed by distillation ($[MgAl_2(OPr^i)_8]$, 120 °C/10^{-2} Torr) or sublimation ($[MgAl_2(OBu^t)_8]$, 140 °C/10^{-2} Torr; and $[MgAl_2(OBu^t)_4H_4]$, 55 °C/10^{-2} Torr) under reduced pressure. Briefly, the isopropoxide compound $[MgAl_2(OPr^i)_8]$ was prepared by the reaction of Mg and Al metal scrapings with isopropyl alcohol in the presence of a small amount of iodine (catalyst).[29] The *tert*-butoxide derivative, $[MgAl_2(OBu^t)_8]$, can be obtained by a salt elimination reaction between $MgCl_2$ and two equivalents of $KAl(OBu^t)_4$.[29] The chemical identity of the precursors was ensured by NMR (^1H and ^{13}C) spectroscopy and elemental analysis (Mg, Al, C, and H). In an alternative synthesis, $[MgAl_2(OPr^i)_8]$ and $[MgAl_2(OBu^t)_8]$ were prepared by reacting $[MgAl_2(OBu^t)_4H_4]$ (eqs 1−3) with excess of isopropyl and *tert*-butyl alcohol, respectively. The NMR data of these products correlates with the earlier reports that confirm the formation of $[MgAl_2(OPr^i)_8]$ and $[MgAl_2(OBu^t)_8]$ (eqs 2 and 3). $[MgAl_2(OPr^i)_8]$ crystallizes as an isopropyl alcohol adduct, $[MgAl_2(OPr^i)_8(Pr^iOH)_2]$, that has been characterized by single-crystal X-ray diffraction analysis to reveal the presence of two coordinated alcohol molecules on the magnesium center,[17] while aluminum atoms display a tetrahedral coordination known for other structurally characterized $MgAl_2X_8$ systems (X = H, Me, OPr^i, OBu^t, $OSiMe_3$).[17] The "alcohol free" compound, $[MgAl_2(OPr^i)_8]$ was obtained by prolonged pumping of a heated (80 °C) sample of isopropyl adduct in dynamic vacuum (10^{-2} Torr) (eq 2) and characterized by chemical analysis.

$$MgCl_2 + 2LiAlH_2(OBu^t)_2 \longrightarrow [MgAl_2(OBu^t)_4H_4] + 2LiCl \quad (1)$$

$$[MgAl_2(OBu^t)_4H_4] + (\text{excess})Pr^iOH \longrightarrow [MgAl_2(OPr^i)_8(Pr^iOH)_2] + 2H_2 \quad (2)$$

$$[MgAl_2(OPr^i)_8(Pr^iOH)_2] \xrightarrow[-2\ Pr^iOH]{\triangle,\ \text{Vacuum}} [MgAl_2(OPr^i)_8]$$

$$[MgAl_2(OBu^t)_4H_4] + (\text{excess})Bu^tOH \longrightarrow [MgAl_2(OBu^t)_8] + 2H_2 \quad (3)$$

(ii) Chemical Vapor Deposition. A cold-wall horizontal CVD system[30,31] operating under reduced pressure was used for the experiments. The reactor was a quartz tube (50 cm long and 4.7 cm o.d.). The substrate (Si or Fe) was placed in the reactor on a graphite susceptor and heated (350−600 °C) inductively using a radio frequency generator. The precursors were introduced in the reactor through a glass flange by applying dynamic vacuum (10^{-4} to 10^{-6} Torr) and maintaining the precursor reservoir at the required temperature (20−125 °C) for an adequate flux. The precursor flux was regulated from the feedback of the pressure measurement in the reactor during the CVD process. Optical pyrometer and a thermocouple monitored the substrate temperature. The thermolysis products and unreacted precursor were removed through the pumping end of the reactor which was connected to rotary vane and turbo molecular vacuum pumps. A quadrupole mass spectrometer was connected to the quartz tube through a metal flange to provide an on-line analysis of the gaseous products or fragments coming out of the reaction zone. Under chosen CVD conditions, the material was deposited selectively on the substrate, and no excessive coating or particle formation was observed on the walls of the reactor.

(iii) Film Characterization. Surface morphology and elemental distribution were recorded in the specimen chamber of a scanning electron microscope JSM-6400F (JEOL) coupled with an energy dispersive X-ray facility (EDX). The film surface topology and average roughness were analyzed with a Topometrix TMX2000 Explorer atomic force microscope (AFM) using a Si_3N_4 standard tip (radius, 20 nm). Film

(16) Sassmannshausen, J.; Riedel, R.; Pflanz, K. B.; Chmiel, H. Z. *Z. Naturforsch.* **1993**, *48*, 7.
(17) Veith, M.; Mathur, S.; Mathur, C. *Polyhedron* **1998**, *17*, 1005.
(18) Veith, M. *J. Chem. Soc., Dalton Trans.* **2002**, 2405.
(19) Veith, M.; Mathur, S.; Shen, H.; Hüfner, S.; Jilavi, M. *Chem. Mater.* **2001**, *11*, 4041.
(20) Veith, M.; Mathur, S.; Lecerf, N.; Bartz, K.; Heintz, M.; Huch, V. *Chem. Mater.* **2000**, *12*, 271.
(21) Jones, A. C. *Chem. Vap. Dep.* **1998**, *4*, 169.
(22) MacInnes, A. N.; Power, M. B.; Barron, A. R. *Chem. Mater.* **1993**, *5*, 1344.
(23) Mathur, S.; Veith, M.; Sivakov, V.; Shen, H.; Huch, V.; Hartmann, U.; Gao, H. B. *Chem. Vap. Dep.* **2002**, *8*, 277.
(24) Cowley, A. H.; Jones, R. A. *Angew. Chem.* **1989**, *101*, 1235.
(25) Lazell, M.; O'Brien, P.; Otway, D. J.; Park, J.-H. *J. Chem. Soc., Dalton Trans.* **2000**, 4479.
(26) Shen, H.; Mathur, S. *J. Phys. IV* 2001, *12*, Pr4−1.
(27) Ihara, M.; Arimoto, Y.; Jifuku, M.; Kimura, T.; Kodama, S.; Yamawaki, H.; Yamaoka, T. *J. Electrochem. Soc.* **1982**, *129*, 2569.
(28) Mathur, S. In *Chemical Physics of Thin Film Deposition Processes for Micro- and Nano-Technologies*; NATO ASI; Kluwer Academic Publishers: Dordrecht, The Netherlands, 2002; p 91.
(29) Bradley, D. C.; Mehrotra, R. C.; Gaur, D. P. *Metal Alkoxides*; Academic Press: London, 1978.
(30) Veith, M.; Kneip, S. *J. Mater. Sci. Lett.* **1994**, *13*, 335.
(31) Veith, M.; Lecerf, N.; Mathur, S.; Shen, H.; Hüfner, S. *Chem. Mater.* **1999**, *11*, 3103.

thickness was measured using optical (spectroscopic ellipsometer ESVG (Sopra)) and mechanical (Profilometer) methods. The phase characterization and texture analysis was done by X-ray diffraction measurements performed on as-deposited films on a STOE diffractometer (STADIP) operating with a Cu Kα radiation. The film composition was determined by electron spectroscopy for chemical analysis (ESCA). The experiments were performed on a Surface Science Instrument, M-Probe, operating with an Al Kα radiation and a total instrumental resolution (fwhm, full width at half-maximum) of ca. 0.8 eV.

Results and Discussion

(i) Precursor Composition and Decomposition Process. From the viewpoint of precursor concept, $[MgAl_2(OPr^i)_8]$, $[MgAl_2(OBu^t)_8]$, and $[MgAl_2(OBu^t)_4H_4]$ are "chemically equivalent" because each of them contains the right proportion of atomic constituents necessary to form the $MgAl_2O_4$ phase. However, their decomposition behavior in the gas phase is governed by the nature of the ligand(s), as a result the decomposition temperatures to obtain crystalline spinel phases are different for the three precursors. Whereas the hydride precursor, $[MgAl_2(OBu^t)_4H_4]$, produces crystalline $MgAl_2O_4$ deposits at temperature as low as 450 °C,[15] substrate temperatures of 600 and 550 °C are necessary to produce crystalline films using $[MgAl_2(OPr^i)_8]$ and $[MgAl_2(OBu^t)_8]$, respectively. It has been reported that vapor transport of $[MgAl_2(OPr^i)_8]$ poses problems, because it tends to oligomerize to other species, such as $[MgAl_2(OPr^i)_8]_2$ and $[Mg_2Al_3(OPr^i)_{13}]$, that are less volatile.[12] We could not confirm these observations as $[MgAl_2(OPr^i)_8]$, in our hands, showed excellent transport properties and adequate stability. It must be noted that the previous studies were made using commercially available $[MgAl_2(OPr^i)_8]$ in which the transport behavior can degrade upon aging. We have used the precursor that is a viscous liquid when freshly distilled. Nevertheless, the molecular framework based on bulkier *tert*-butoxide ligands in $[MgAl_2(OBu^t)_8]$ is thermally more robust and can be used for the deposition of stoichiometric spinel films, however the increased molecular weight of the compound and bulkier alkoxy groups seem to hamper its volatility. Although alkoxy ligands with increased steric profile are expected to increase the volatility by reducing the nuclearity, this effect is not apparent in the case of $[MgAl_2(OBu^t)_8]$ because the overall framework in the three monomeric precursors is comparable. In addition, the increased thermal stability necessitates high decomposition temperatures. In the context of precursor properties, $[MgAl_2(OPr^i)_8]$ (liquid) is more suitable than $[MgAl_2(OBu^t)_8]$ (solid). Liquid source compounds are desirable in a CVD process, because they offer a constant flux through an unchanged surface area (exposed meniscus). By contrast, the surface area of a solid precursor changes with decreasing amount of precursor, consequently leading to variable concentration in the gaseous precursor stream.

The isopropoxide compound, $[MgAl_2(OPr^i)_8(Pr^iOH)_2]$, has been used for the synthesis of ultrafine spinel particles by sol−gel method.[32] The hydrolysis of the heterometal precursor was investigated by rheological measurements and ^{27}Al NMR spectroscopy, which suggested that the bimetallic unit survives during hydrolysis and gelation, and does not break down to constituent alkoxides.[32] For the gas-phase technique, molecules containing coordinated neutral ligands are not suitable precursors because the adduct solvent molecules can be knocked off (due to weaker bonding) under low-pressure conditions creating an unsaturated metal center that may trigger the oligomerization of the precursor and reduce the vapor pressure. For this reason, significant efforts are being made to tailor the nuclearity and structural stability of the precursor compounds.[33−37] Kim et al. have synthesized alkyl-modified alkoxides $[MgAl_2(OPr^i)_4Me_4]$[38] and $[MgAl_2(OBu^t)_4Me_4]$[38] by replacing the terminal alkoxide ligands present on aluminum atoms through methyl groups. Both the precursors are much more volatile than $MgAl_2(OR)_8$ compounds; $Mg[(O^iPr)_2AlMe_2]_2$ can be vapor-transported at room temperature, whereas $Mg[(O^tBu)_2AlMe_2]_2$ should be heated to 60 °C. The isopropoxide precursor, $[MgAl_2(OPr^i)_4Me_4]$, showed better transport properties due to the reduction in molecular weight, however the spinel films obtained were largely amorphous at 600 °C and needed annealing at 900 °C in air for the phase evolution. This shows that precursor design is case-dependent and not always an advantage, because the simple Mg−Al isopropoxide complex, $[MgAl_2(OPr^i)_8]$, is sufficiently volatile and provides crystalline deposits of $MgAl_2O_4$ at 600 °C.

Veith et al. have introduced a more elegant design in which the terminal alkoxide ligands on Al centers were replaced by hydride ligands[15] to obtain the hydride-modified Mg−Al *tert*-butoxide, $[MgAl_2(OBu^t)_4H_4]$. As a consequence of the drastic reduction in the molecular weight, an enhanced volatility is observed for the modified precursors ($[MgAl_2(OBu^t)_8]$, 100 °C; $[MgAl_2Me_4(OBu^t)_4]$, 60 °C; $[MgAl_2H_4(OBu^t)_4]$, 45 °C). Both alkyl and hydride modifications, generally speaking, are based on the abstraction of β-hydrogen (by an incipient carbanion) from the alkoxy group to eliminate methane ($[MgAl_2Me_4(OBu^t)_4]$) or dihydrogen ($[MgAl_2H_4(OBu^t)_4]$) and iso-butene. This principle of organometallic chemistry has already been exploited for the deposition of ZnO and MgO from methyl zinc alkoxide and methylmagnesium alkoxide, respectively.[39] However, this strategy is not effective in designing a precursor to zinc gallate ($ZnGa_2O_4$). The Zn−Ga compound $[ZnGa_2Me_4(OPr^i)_4]$ is thermally labile and disproportionates under the CVD conditions to give dimethyl gallium isopropoxide and zinc isopropoxide, the latter being nonvolatile.[40]

(32) Jones, K.; Davies, T. J.; Emblem, H. G.; Parks, P. *Mater. Res. Soc. Symp. Proc.* **1986**, *73*, 111.

(33) Jones, A. C.; Davies, H. O.; Leedham, T. J.; Wright, P. J.; Crosbie, M. J.; Steiner, A.; Bickley, J. F.; O'Brien, P.; White, A. J. P.; Wiliams, D. J. *J. Mater. Chem.* **2001**, *11*, 544.

(34) Crosbie, M. J.; Wright, P. J.; Davies, H. O.; Jones, A. C.; Leedham, T. J.; O'Brien, P.; Critchlow, G. W. *Chem. Vap. Dep.* **1999**, *5*, 9.

(35) Davies, H. O.; Jones, A. C.; Leedham, T. J.; Wright, P. J.; Crosbie, M. J.; Lane, P. A.; Steiner, A.; Bickley, J. F. *Adv. Mater. Opt. Electron.* **2000**, *10*, 177.

(36) Hubert-Pfalzgraf, L. G. *Polyhedron* **1994**, *13*, 1181.

(37) Chunggaze, M.; Malik, M. A.; O'Brien, P. *Adv. Mater. Opt. Electron.* **1998**, *7*, 311.

(38) Boo, J. H.; Lee, S. B.; Ku, S. J.; Koh, W.; Kim, C.; Yu, K. S.; Kim, Y. *Appl. Surf. Sci.* **2001**, *169−170*, 581.

(39) Auld, J.; Houlton, D. J.; Jones, A. C.; Rushworth, S. A.; Malik, M. A.; O'Brien, P.; Critchlow, G. W. *J. Mater. Chem.* **1994**, *4*, 1249.

(40) Kim, C. G.; Koh, W.; Ku, S. J.; Nah, E. J.; Yu, K. S.; Kim, Y. *J. Phys. IV* **1999**, *9*, Pr8−853.

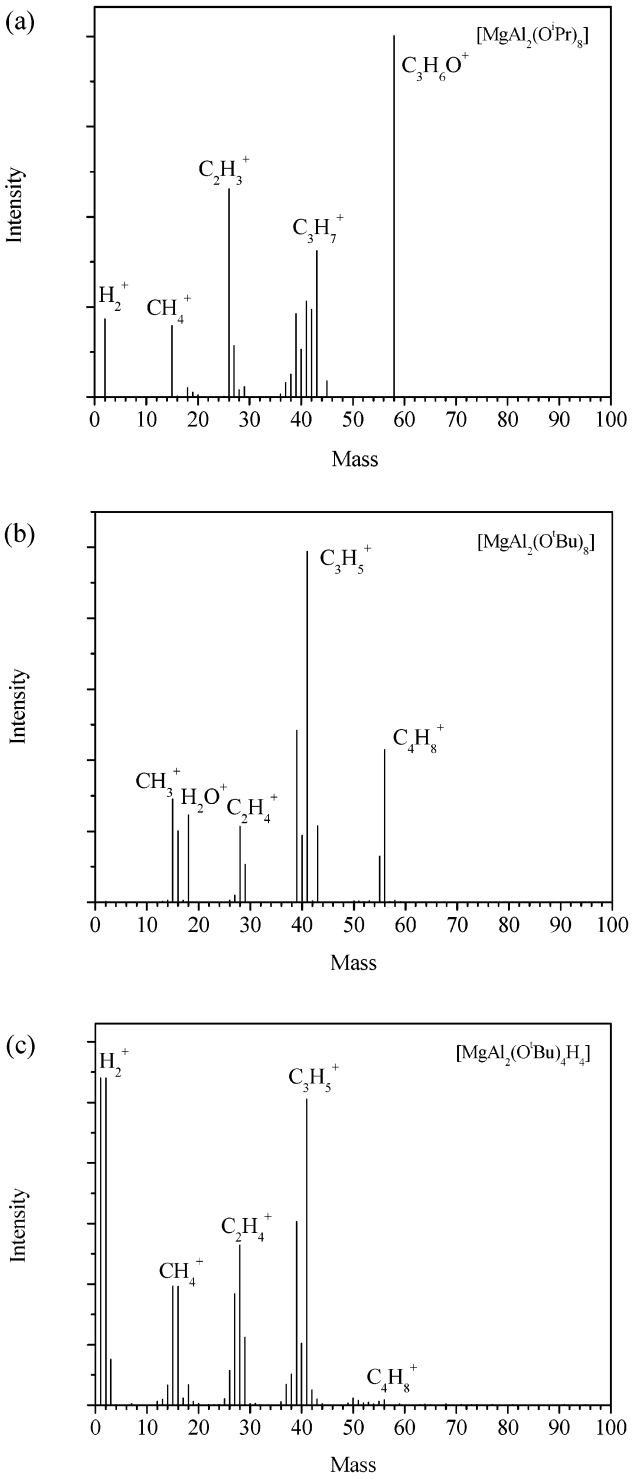

Figure 1. Mass spectra of volatile reaction products detected in the CVD of (a) **MA1**, (b) **MA2** and (c) **MA3**.

The gas-phase pyrolysis of the precursors $[MgAl_2(OPr^i)_8]$, $[MgAl_2(OBu^t)_8]$, and $[MgAl_2(OBu^t)_4H_4]$ was performed as described in the Experimental Section. The structural characterization of the precursors[12,14−17] confirms the presence of an appropriate Mg:Al ratio, in all the three cases, necessary for the formation of a stoichiometric spinel phase. However, they show different vapor pressure characteristics depending upon their molecular weight and nature of the ligands.

The on-line mass spectrometric (MS) analysis (Figure 1) of the residual gases gives clues for a possible decomposition profile of individual precursors. The major species (Figure 1a) detected in the CVD of $[MgAl_2(OPr^i)_8]$ are fragments of isopropyl alcohol and acetone. This was confirmed by recording the mass spectral patterns of isopropyl alcohol and acetone under identical conditions followed by a differential peak analysis of the MS data recorded during the CVD of $[MgAl_2(OPr^i)_8]$. Further, the results observed correlate to the mass spectral data recorded during the CVD of other isopropoxide precursors.[19,20]

The observation of other species (water, propene) in the mass spectra is due to the fact that products eliminated during the first step of decomposition of the molecular precursor (primary reaction) undergo further fragmentation (secondary reactions) to produce different species whose composition and concentration depend on the process temperature. For example, isopropyl alcohol can decompose on a hot aluminum oxide surface, subject to the local temperature, through dehydration or dehydrogenation reactions, to produce propene or acetone, respectively.[41] These reactions are obviously accompanied by the formation of water, molecular hydrogen, and isopropene (eq 4). These species can either react with the precursor (e.g., hydrolysis of the precursor by H_2O, formed in the dehydration of Pr^iOH) or incorporate in the film material (e.g., elemental carbon formed by the reduction or pyrolysis of the organic compounds). Therefore, for an efficient decomposition process, a precisely defined temperature window should be coupled with an efficient removal of the gaseous byproducts from the deposition zone.

$$[MgAl_2(OPr^i)_8] \longrightarrow \quad (\mathbf{MA1})$$

$$MgAl_2O_4 + (CH_3)_2CHOH + (CH_3)_2C{=}O + (CH_3)HC{=}CH_2 + H_2 + H_2O \qquad (4)$$

$$[MgAl_2(OBu^t)_8] \longrightarrow \quad (\mathbf{MA2})$$

$$MgAl_2O_4 + (CH_3)_3COH + (CH_3)_2C{=}CH_2 + CH_4 + H_2O \qquad (5)$$

$$[MgAl_2(OBu^t)_4H_4] \longrightarrow \quad (\mathbf{MA3})$$

$$MgAl_2O_4 + (CH_3)_2C{=}CH_2 + H_2 \qquad (6)$$

In contrast to metal isopropoxides compounds, the decomposition of metal *tert*-butoxides is relatively simple and shows *tert*-butyl alcohol, isobutene, and water to be the major gas-phase products as found in the case of $[MgAl_2(OBu^t)_8]$ (eq 5). The origin of water lies in the dehydration of Bu^tOH to produce iso-butene and water. As a result, the overall amount of iso-butene observed in the decomposition of $[MgAl_2(OBu^t)_8]$ is less than that found in $[MgAl_2(OBu^t)_4H_4]$ because it contains only 4 against 8 $-OBu^t$ groups in $[MgAl_2(OBu^t)_8]$ (Scheme 1). The decomposition mechanism in $[MgAl_2(OBu^t)_4H_4]$ is based on β-hydrogen elimination in which one of the protons of the *tert*-butyl moiety migrates to the hydride

(41) Chang, C. C.; Lee, W. H.; Her, T. Y.; Lee, G. H.; Peng, S. M.; Wang, Y. *J. Chem. Soc., Dalton Trans.* **1994**, 315.

Scheme 1. Possible Ligand Elimination Mechanisms in the Thermolytic Decomposition of $[MgAl_2(OPr^i)_8]$, $[MgAl_2(OBu^t)_8]$, and $[MgAl_2(OBu^t)_4H_4]$

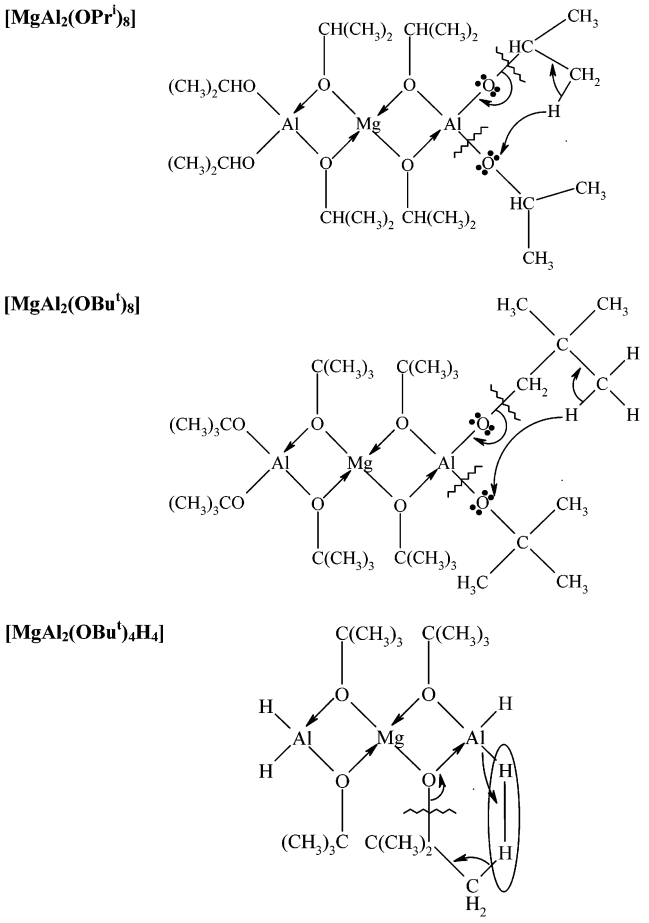

ligand present on Al centers to facilitate the formation of molecular hydrogen, while the rest of the organic part is eliminated as isobutene molecules (eq 6).[15] In the case of $[MgAl_2(OPr^i)_8]$ and $[MgAl_2(OBu^t)_8]$, the protonation of one of the alkoxy oxygen atoms (alcohol formation) and the C−O bond fission (alkene elimination) are competitive reactions, whereas in $[MgAl_2(OBu^t)_4H_4]$ the presence of terminal hydride ligands compels a β-hydride elimination. Formation of *tert*-butyl alcohol is not observed, because this would require the abstraction of oxygen bonded to two electropositive metal centers and therefore energetically unfavorable. Nevertheless, if the elimination of isobutene is the first step in the decomposition reaction, a metal-bound hydroxy group will be left in the precursor framework after the migration of a protic hydrogen to the alkoxide oxygen with a concomitant elimination of C_4H_8 molecule (Scheme 1). Such an intermediate can react with other molecules to produce either water or *tert*-butyl alcohol by condensation reactions. The plausible ligand elimination mechanisms active in the decomposition of $[MgAl_2(OPr^i)_8]$, $[MgAl_2(OBu^t)_8]$, and $[MgAl_2(OBu^t)_4H_4]$ are represented in Scheme 1 and eqs 4−6. The molecular structures are drawn on the basis of the single-crystal X-ray diffraction data reported for the precursor molecules.[15,17]

(ii) Film Growth and Characterization. The scanning electron micrographs of films deposited on iron substrates using $[MgAl_2(OPr^i)_8]$, $[MgAl_2(OBu^t)_8]$, and

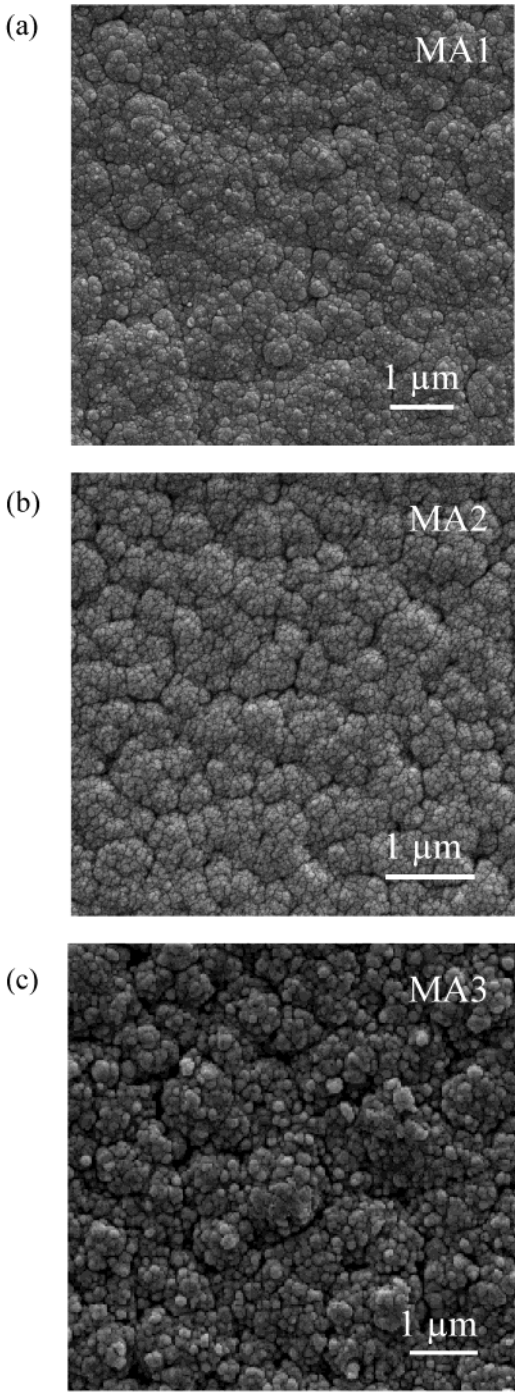

Figure 2. Scanning electron micrographs (a−c) of the $MgAl_2O_4$ films deposited on Fe at 550 °C using **MA1**, **MA2**, and **MA3**, respectively.

$[MgAl_2(OBu^t)_4H_4]$ in the CVD process at 550 °C show a granular morphology formed by homogeneous agglomerates of spherical nodules (Figure 2). Despite the same deposition temperature, the average particle size is different in the three films. The film obtained from precursor $[MgAl_2(OBu^t)_8]$ contains the smallest particles, whereas much larger grains are observed in the other two samples. This trend in the film morphology was confirmed by atomic force micrographs that show an increase in the surface roughness in the order $[MgAl_2(OBu^t)_4H_4] > [MgAl_2(OPr^i)_8] > [MgAl_2(OBu^t)_8]$.

Figure 3 shows the influence of substrate temperature (T_S) on the roughness of $MgAl_2O_4$ films obtained from

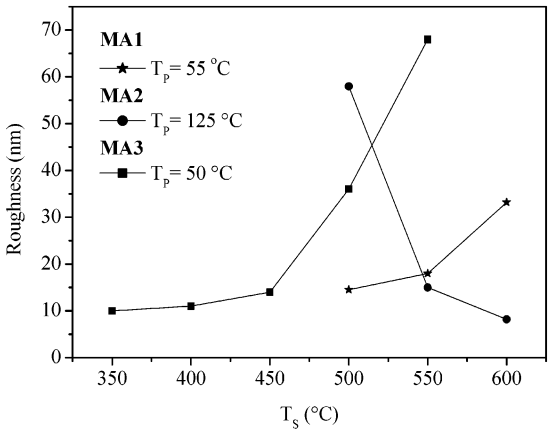

Figure 3. Surface rms-roughness of spinel films on Fe deposited at different substrate temperatures using **MA1**, **MA2**, and **MA3**.

$[MgAl_2(OPr^i)_8]$, $[MgAl_2(OBu^t)_8]$, and $[MgAl_2(OBu^t)_4H_4]$ precursors in which the precursor temperature (T_P) was kept constant at 55, 125, and 50 °C, respectively. The surface roughness in films obtained from $[MgAl_2(OBu^t)_8]$ decreased when the substrate temperature was increased, possibly due to increased mobility of the surface species at higher temperatures. In contrast, the roughness was found to increase with increasing substrate temperature in the films obtained from $[MgAl_2(OPr^i)_8]$ and $[MgAl_2(OBu^t)_4H_4]$. Apparently, the surface chemistry is fast in the case of $[MgAl_2(OPr^i)_8]$ and $[MgAl_2(OBu^t)_8]$ so that the deposition rate is limited by the ability of the gas-phase species to be transported by molecular diffusion process through the gas-phase boundary layer adjacent to the deposition surface (transport limited). However, in the case of $[MgAl_2(OBu^t)_4H_4]$, the transport rate is significantly higher and the growth is limited by surface reactions (surface limited). This is conceivable in light of the different sublimation temperatures of $[MgAl_2(OBu^t)_8]$ (140 °C/10^{-2} Torr) and $[MgAl_2(OBu^t)_4H_4]$ (55 °C/10^{-2} Torr). The AFM analyses of films deposited using $[MgAl_2(OBu^t)_4H_4]$ at different substrate and precursor temperatures suggest that the decomposition rate of $[MgAl_2(OBu^t)_4H_4]$ is slower than the incoming precursor flux. As a result, the nucleation density is too high, which hinders the surface mobility and favors island growth, thus giving rough surfaces even at higher substrate temperatures. A profound influence on the film roughness was observed (Figure 4) on varying the substrate temperature from 450 to 550 °C. For instance, at constant precursor temperature (50 °C), the root-mean-square (rms)-roughness of the film ranges between 10 and 15 nm at 450 °C, but reaches 65−70 nm at 550 °C (Figure 4). On the other hand, a variation in precursor flux had no effect on the basic film morphology and average roughness values. The film deposited at precursor temperatures of 50 and 60 °C gave rms-roughness values of 10 and 15 nm, respectively.

The cross-sectional analysis (Figure 5) of the films deposited using the three precursors on silicon shows a directed growth and formation of columnar structures normal to the substrate. Close to the interface of substrate and spinel film the layer possesses higher density than in the upper region of the film, which may occur due to a change in growth mechanism at a certain point of film evolution. The columnar microstructure observed here is of considerable interest for the application of $MgAl_2O_4$ films as thermal insulators, because the problems (spallation, cracks, etc.) induced at the substrate−film interface by thermal stresses can be reduced in a columnar microstructure that would prevent crack propagation.[4] When compared to $MgAl_2O_4$ films obtained from $[MgAl_2(OPr^i)_8]$ and $[MgAl_2(OBu^t)_8]$, the films deposited from $[MgAl_2(OBu^t)_4H_4]$ exhibit less dense and noncolummar microstructure probably due to a very high deposition rate (high nucleation density) that leads to a particulate growth and a considerable amorphous content as indicated by the XRD data.

The X-ray diffraction patterns of the films deposited on iron using $[MgAl_2(OPr^i)_8]$ and $[MgAl_2(OBu^t)_8]$ at 550 °C and $[MgAl_2(OBu^t)_4H_4]$ at 450 °C are shown in Figure 6. The diffraction profiles of films deposited using $[MgAl_2(OPr^i)_8]$ at a substrate temperature of 550 °C show a short-range ordering supported by two broad peaks. However, $MgAl_2O_4$ films grown from $[MgAl_2(OBu^t)_8]$ at 550 °C show a crystalline $MgAl_2O_4$ phase with average particle size (Scherer Formula) being ca. 6−8 nm. However, only amorphous deposits were obtained when the substrate temperature was kept

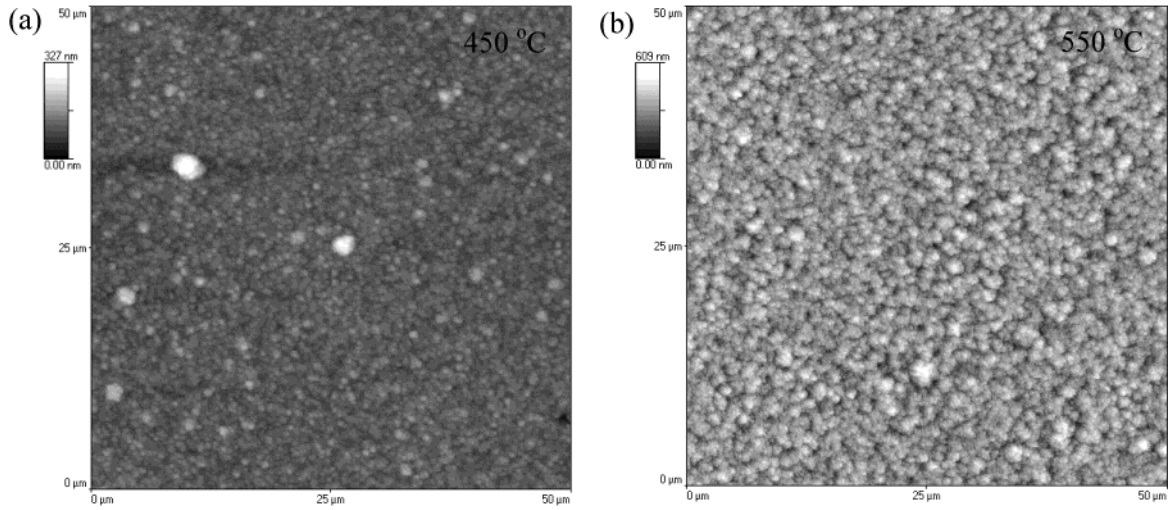

Figure 4. AFM images of spinel films on Fe using **MA3** precursor heated at 50 °C at substrate temperatures of (a) 450 and (b) 550 °C.

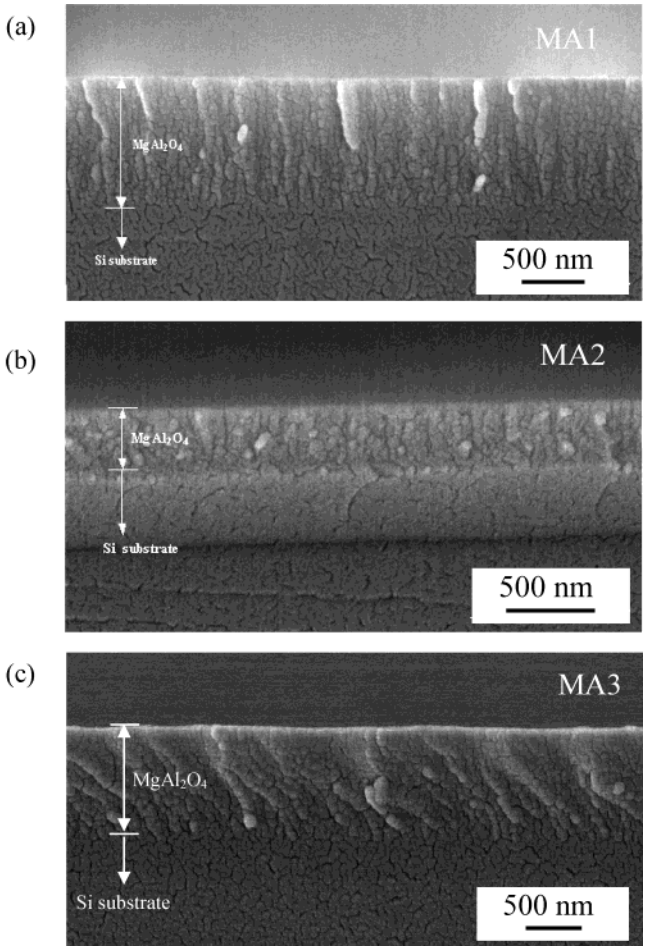

Figure 5. Cross-sectional SEM images of spinel films on silicon obtained from (a) **MA1**, (b) **MA2**, and (c) **MA3**.

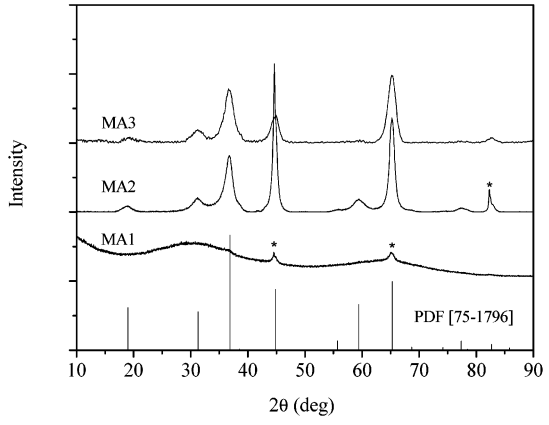

Figure 6. XRD profiles of $MgAl_2O_4$ films on Fe (*) deposited from (a) **MA1** (550 °C), (b) **MA2** (550 °C), and (c) **MA3** (450 °C).

below 500 °C. In comparison to $[MgAl_2(OPr^i)_8]$ and $[MgAl_2(OBu^t)_8]$, $[MgAl_2(OBu^t)_4H_4]$ offers crystalline CVD deposits at 450 °C with an average particle size being ca. 4−5 nm. Although all three precursors deliver the atomic constituents necessary to form the spinel phase, the crystallization process is different in each case. Evidently, the formation of a crystalline solid phase from a metal−organic source is sensitive to molecular thermochemistry and single molecule processes active on the substrate surface (e.g., fragmentation or recombination of the gaseous species, reactivity, mobility, and

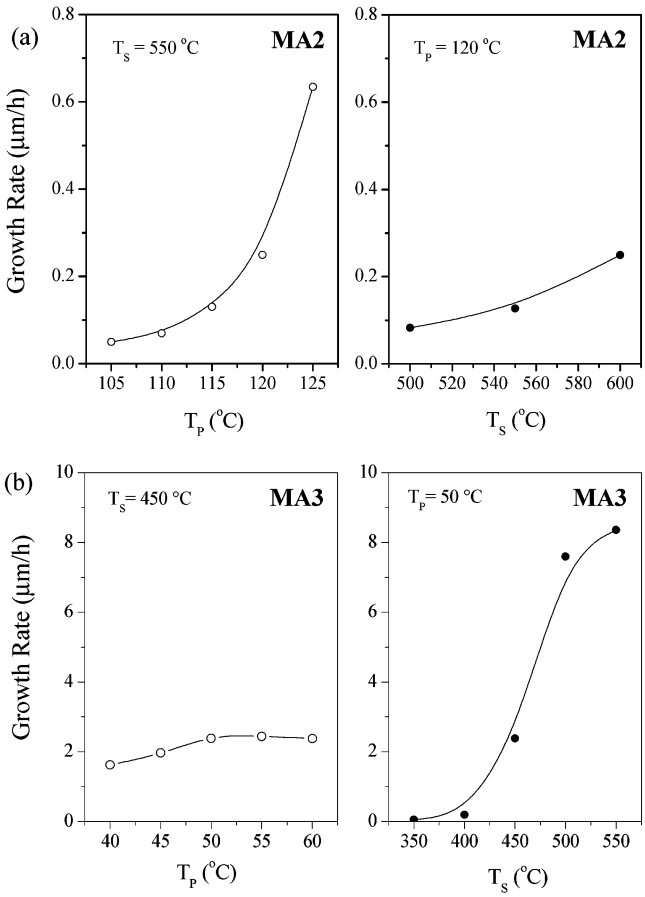

Figure 7. Influence of substrate (Fe) temperature and precursor flux on the growth rate in the case of (a) **MA2** and (b) **MA3** precursors.

collisional stability of the gas-phase species produced after partial and/or complete ligand stripping). The results obtained using $[MgAl_2(OPr^i)_8]$, $[MgAl_2(OBu^t)_8]$, and $[MgAl_2(OBu^t)_4H_4]$ demonstrate that an effective ligand elimination mechanism and low decomposition temperature (low activation barrier) of the gas-phase species generated from $[MgAl_2(OBu^t)_4H_4]$ make it an *efficient and benevolent* precursor for growing crystalline spinel films at low temperatures.

The film thickness of the CVD deposits was determined using ellipsometry and a mechanical profilometer for thin and thick films, respectively. Using $[MgAl_2(OPr^i)_8]$, growth rates ranging from 0.24 to 0.57 μm/h were observed at substrate and precursor temperatures of 550 and 75 °C, respectively. Higher growth rates of several micrometers per hour could be achieved by increasing the precursor flux. On the other hand, the presence of bulkier ligands and higher melting point in $[MgAl_2(OBu^t)_8]$ ($[MgAl_2(OPr^i)_8]$ is a liquid) reduces the vapor pressure of the molecule; as a result much higher precursor temperatures were necessary to obtain comparable growth rates. Figure 7 displays the influence of precursor and substrate temperature on the film thickness obtained from $[MgAl_2(OBu^t)_8]$ and $[MgAl_2(OBu^t)_4H_4]$. In the CVD of $[MgAl_2(OBu^t)_8]$, the substrate temperature marginally influences film thickness; however, a remarkable enhancement was observed on varying the precursor temperature. For example, the growth rate (0.25 μm/h) at a precursor temperature of 120 °C showed almost 3-fold increase (0.65 μm/h) when

the precursor temperature was enhanced to 125 °C. This observation indicates a transport limited growth in the case of $[MgAl_2(OBu^t)_8]$. The deposition kinetics of $[MgAl_2(OBu^t)_4H_4]$ is different from the other two precursors due to its high vapor pressure (20 °C/10^{-2} Torr) and low decomposition temperature (350 °C). Because the decomposition of $[MgAl_2(OBu^t)_4H_4]$ is surface limited, no significant changes in the film thickness were observed on changing the precursor temperature in the range 40−60 °C. However, the substrate temperature plays a major role in triggering the surface reactions. Consequently, growth rates could be improved from 2.5 μm/h (450 °C) to 8.5 μm/h (550 °C) by increasing the substrate temperature.

To estimate the element distribution and carbon contamination in $MgAl_2O_4$ films obtained from $[MgAl_2(OPr^i)_8]$, $[MgAl_2(OBu^t)_8]$, and $[MgAl_2(OBu^t)_4H_4]$, depth profiles were recorded using X-ray photoelectron spectroscopy. Films were gradually sputtered by Ar^+ treatment under similar experimental conditions. Figure 8 shows the consistency of element distribution and the amount of carbon incorporated in the film during the deposition process. The results indicate that the films deposited using $[MgAl_2(OPr^i)_8]$ contained minimum carbon contamination (ca. 2.7 atom %), whereas the carbon contents in the films obtained from $[MgAl_2(OBu^t)_8]$ and $[MgAl_2(OBu^t)_4H_4]$ were found to be 3.5 and 5 atom %, respectively. In comparison to $[MgAl_2(OPr^i)_8]$, the more carbon within the $[MgAl_2(OBu^t)_8]$ thin film is attributed to the higher number of carbon atoms present in the $[MgAl_2(OBu^t)_8]$ precursor (32 versus 24 C atoms, in $[MgAl_2(OPr^i)_8]$). The origin of higher carbon content in the films obtained using $[MgAl_2(OBu^t)_4H_4]$ might be due to much higher vapor pressure that leads to mass transport higher than the rate of surface reactions. As a result, partially decomposed precursor or organic byproduct embeds in the film material during the film's growth. The Al/Mg ratios determined from the XPS data reveal that the theoretical value (Al/Mg = 2) is achieved in films deposited using $[MgAl_2(OBu^t)_8]$ (Figure 9), whereas a small deviation (~0.2) in the Al:Mg ratio is observed in films obtained from $[MgAl_2(OPr^i)_8]$ and $[MgAl_2(OBu^t)_4H_4]$ which shows a slight deficiency of Al in the films.

Given the application potential of $MgAl_2O_4$ thin films as humidity sensors and the fact that the adsorption and the capillary condensation of water affect the electrical properties of ceramic films, the resistance of spinel films was measured. As-obtained samples stored under ambient conditions exhibit a significant uptake of atmospheric moisture that increases the conductivity of the samples (Figure 10). After a drying step (oven, 120 °C, 12 h) undertaken to remove the adsorbed water, the film resistance was found to increase. The relative change in the resistance value is attributed to mobile protons dissociated from the hydroxyl groups of adsorbed water molecules. The relative large variation of absolute resistance in as-deposited and dried spinel films, obtained from $[MgAl_2(OBu^t)_4H_4]$, is apparently due to the morphology of the films. The porous microstructure and nanostructured surface offer a large amount of water to be adsorbed on the surface and in the pores of the films (Figure 5c) which increases the conductivity of the films. Remarkably, the resistance

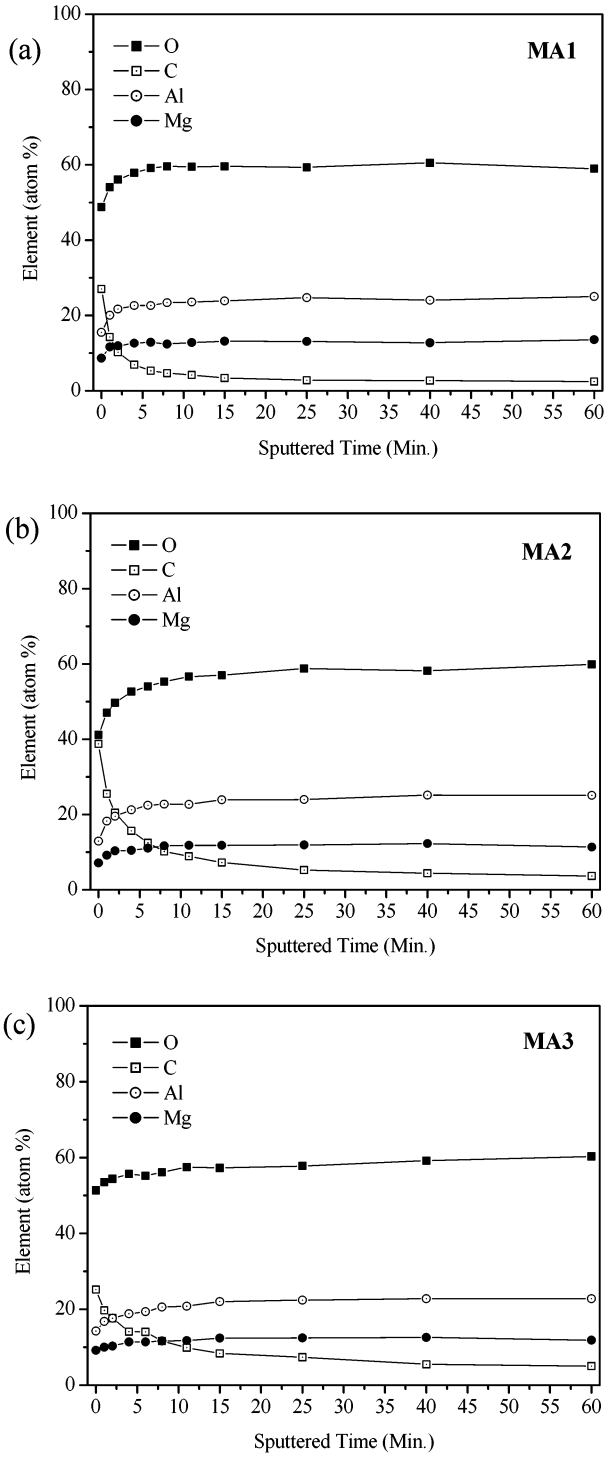

Figure 8. Depth profiles of $MgAl_2O_4$ thin films on Fe obtained from (a) **MA1**, (b) **MA2**, and (c) **MA3**.

value expected for a dielectric oxide can be achieved by drying the film at 120 °C and is found to be even higher than that for films obtained from $[MgAl_2(OPr^i)_8]$ and $[MgAl_2(OBu^t)_8]$. The evaluation of precursor and spinel properties (Table 1) shows that several chemical parameters influence the precursor design that is ultimately responsible for the properties of the resulting material. An efficient precursor results from the tradeoff among different attributes such as ease of preparation, long-term stability, vapor pressure, gas-phase stability, decomposition temperature, and ligand elimination mechanism (random or designed).

Table 1. Important Data Related to the Properties of Precursors and CVD Deposits

precursor	vapor pressure	decomposition temperature	residual carbon	crystallinity of deposit	stoichiometry control	growth rate
$[MgAl_2(O^iPr)_8]$(**MA1**)	satisfactory	high	low	poor	acceptable	good
$[MgAl_2(O^iBu)_8]$(**MA2**)	low	high	marginal	good	good	low
$[MgAl_2H_4(O^iBu)_4]$(**MA3**)	high	low	marginal	satisfactory	acceptable	high

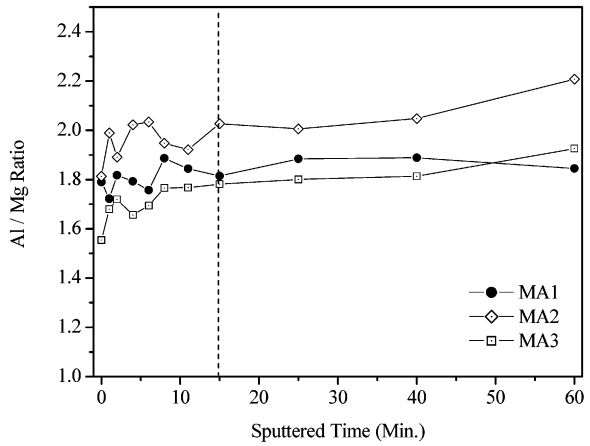

Figure 9. Consistency of Al:Mg ratio in $MgAl_2O_4$ films on Fe obtained from (a) **MA1**, (b) **MA2**, and (c) **MA3**.

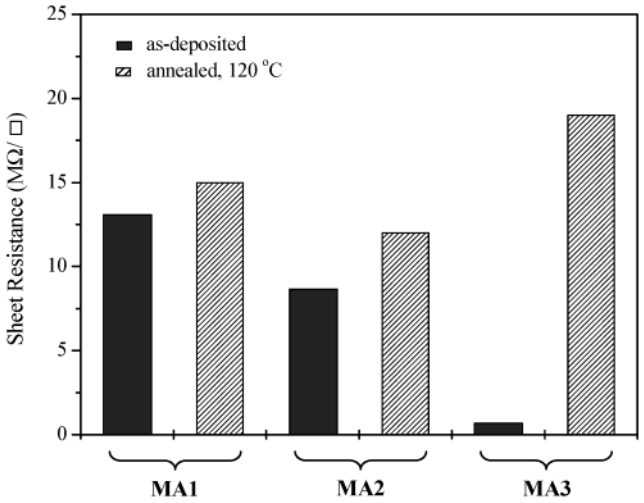

Figure 10. Sheet resistance of $MgAl_2O_4$ films on silicon obtained from (a) **MA1**, (b) **MA2**, and (c) **MA3**.

Conclusions

$MgAl_2O_4$ thin films were deposited in a low-pressure CVD process using $MgAl_2(OPr^i)_8$ (**MA1**), $MgAl_2(O^tBu)_8$ (**MA2**), and $MgAl_2H_4(O^tBu)_4$ (**MA3**) as precursors. Because all the compounds fulfill the essential criterion of molecular sources (Mg:Al ratio compatible to $MgAl_2O_4$), films with spinel composition could be grown in all the cases. A comparative analysis of the deposition parameters and characterization of the deposits reveal that decomposition chemistry ultimately determines the deposition temperature, crystallinity, morphology, and phase purity of the CVD deposits. We could not confirm the tendency of $[MgAl_2(OPr^i)_8]$ to oligomerize in the gas phase or in an aged sample and the following adverse effects on the vapor pressure and stoichiometry of the film. In contrast, $[MgAl_2(OPr^i)_8]$ showed adequate vapor pressure, and films obtained were stoichiometric with a columnar microstructure. The *tert*-butoxide analogue, $[MgAl_2(OBu^t)_8]$, is thermally and structurally more stable due to the presence of larger *tert*-butoxy ligands, however, they cause higher molecular weight which lowers the vapor pressure of the molecule. As a result, high precursor temperature is necessary to achieve adequate growth rates. $[MgAl_2(OBu^t)_4H_4]$ represents a precursor modified by a judicious choice of a ligand combination ($-H^-/-O^tBu^-$) that endows a designed ligand elimination mechanism in the molecule based on β-hydrogen elimination. This modification enhances the volatility of $[MgAl_2(OBu^t)_4H_4]$ and lowers the deposition temperature when compared to $[MgAl_2(OPr^i)_8]$ and $[MgAl_2(OBu^t)_8]$. Consequently, high feeding rates could be achieved using $[MgAl_2(OBu^t)_4H_4]$; however, they cause higher carbon contamination in the films at high fluxes. The experimental data support the above remarks, as substrate temperatures of 550 and 600 °C are necessary to obtain spinel deposits using $[MgAl_2(OBu^t)_8]$ and $[MgAl_2(OPr^i)_8]$, respectively, whereas crystalline films are obtained at 450 °C when $[MgAl_2(OBu^t)_4H_4]$ is used as the precursor. Similarly, the lower vapor pressures of $[MgAl_2(OPr^i)_8]$ and $[MgAl_2(OBu^t)_8]$ demand higher temperatures for the precursor reservoir to achieve appreciable growth rates, whereas the precursor temperature shows no important influence on the film thickness in the case of $[MgAl_2(OBu^t)_4H_4]$.

This work underlines the importance of precursor chemistry on the performance of the final nanomaterial and demonstrates that suitability of a precursor is subject to several chemical parameters such as vapor pressure, structural and thermal stability, association tendency, nature of ligands, and chemical behavior of the participating ions, etc.

Acknowledgment. We are thankful to the Saarland state and central government for providing financial assistance. Thanks are due to the German Science Foundation (DFG) for supporting this work in the frame of the priority program on nanomaterials − *Sonderforschungsbereich 277* − operating at the Saarland University, Saarbruecken, Germany.

CM0311675